Current Biology 20, 934–938, May 25, 2010 ©2010 Elsevier Ltd All rights reserved DOI 10.1016/j.cub.2010.03.060

Report

A Distance-Weighted Interaction Map Reveals a Previously Uncharacterized Layer of the *Bacillus subtilis* Spore Coat

Peter T. McKenney,[1] Adam Driks,[2] Haig A. Eskandarian,[1,4] Paul Grabowski,[1,5] Jonathan Guberman,[3] Katherine H. Wang,[1,6] Zemer Gitai,[3] and Patrick Eichenberger[1,*]

[1]Center for Genomics and Systems Biology, Department of Biology, New York University, New York, NY 10003, USA
[2]Department of Microbiology and Immunology, Loyola University Medical Center, Maywood, IL 60153, USA
[3]Department of Molecular Biology, Princeton University, Princeton, NJ 08540, USA

Summary

Bacillus subtilis **spores are encased in a protein assembly called the spore coat that is made up of at least 70 different proteins. Conventional electron microscopy shows the coat to be organized into two distinct layers. Because the coat is about as wide as the theoretical limit of light microscopy, quantitatively measuring the localization of individual coat proteins within the coat is challenging. We used fusions of coat proteins to green fluorescent protein to map genetic dependencies for coat assembly and to define three independent subnetworks of coat proteins. To complement the genetic data, we measured coat protein localization at subpixel resolution and integrated these two data sets to produce a distance-weighted genetic interaction map. Using these data, we predict that the coat comprises at least four spatially distinct layers, including a previously uncharacterized glycoprotein outermost layer that we name the spore crust. We found that crust assembly depends on proteins we predicted to localize to the crust. The crust may be conserved in all *Bacillus* spores and may play critical functions in the environment.**

Results and Discussion

The integration of complementary data types has been important in elucidating the structural organization of multiprotein assemblies with sizes that are near the theoretical limit of resolution of light microscopy [1]. Data integration has produced high-resolution models of the yeast nuclear pore complex, the kinetochore, and clathrin-coated vesicles [2–4]. Using the protein visualization tools of cell biology and light microscopy, it is a relatively simple matter, even in bacterial cells [5], to investigate the subcellular localization of individual proteins to various structures, such as the flagellum [6], the divisome [7], or the genetic transformation machinery [8]. Gaining additional information about the arrangement of individual proteins that appear colocalized by fluorescence light microscopy has become possible with new techniques that enable resolution far below the theoretical limit of 200 nm [9]. Although very promising these techniques are still in their infancy and, until recently, required custom-built optics systems. Although immunoelectron microscopy (immuno-EM) can convincingly localize individual proteins to specific spatial subregions of multiprotein assemblies [10, 11], it suffers from low sensitivity and poor structural preservation. An alternative has emerged with high-resolution image analysis of conventional fluorescence microscopy images [4, 12, 13]. This approach provides resolution beyond mere colocalization of proteins without sacrificing the advantages of working with live cells. Here, we describe a novel integrated approach to identify the architecture of a large multiprotein structure, the spore coat of *Bacillus subtilis*, at an effective resolution below the theoretical limit of resolution of light microscopy.

B. subtilis can form highly resistant spores in response to adverse conditions. A division septum is placed toward one end of the sporulating cell, dividing it into two membrane-bounded compartments [14]. The smaller compartment, the forespore, becomes the spore. Two major protective structures are layered concentrically around the spherical core: the cortex (spore peptidoglycan) and the coat [15, 16]. However, some species possess an additional outermost protective layer called the exosporium [15, 17]. In *B. subtilis*, the coat is made up of at least 70 individual proteins synthesized in the larger mother cell compartment and deposited onto the spore surface. Thin-section transmission EM shows that the coat is organized into distinct inner and outer layers [18].

The *B. subtilis* Spore Coat Genetic Interaction Network

Assembly of the spore coat is controlled by a subset of coat proteins, known as the morphogenetic proteins [15, 16]. The locations of morphogenetic proteins within the coat have been inferred from a combination of genetic and EM analyses. In the *spoIVA* mutant, the coat fails to localize to the spore [19]. Because SpoIVA interacts directly with SpoVM, a peptide that localizes to positively curved membrane surfaces [20], SpoIVA and SpoVM are inferred to be at the top of the genetic hierarchy. Immuno-EM shows CotE at the interface of the inner and outer layers, and *cotE* mutant spores lack the outer coat. Thus, CotE is inferred to be in the middle of the genetic hierarchy [10, 21].

It is possible to determine genetic dependencies of individual coat proteins in deletion mutants of morphogenetic proteins by using coat proteins fused to the green fluorescent protein (GFP) [22, 23]. Using this molecular epistasis approach, we generated a genetic interaction network that incorporates 40 proteins [23, 24] (see Table S1 available with this article online). In previous work and as shown in Figure S1, we identified 16 coat protein-GFP fusions that are dependent on *cotE* for localization; therefore, we classified them as outer coat proteins [23].

CotE functions as an interaction hub protein for the outer coat; however, no equivalent protein has been identified for the inner coat. A strong candidate is SafA. EM analysis shows that *safA* mutant spores possess a defective inner coat, and immunogold labeling indicates that SafA resides at

*Correspondence: pe19@nyu.edu
[4]Present address: Unité des Interactions Bactéries-Cellules, Institut Pasteur, Paris F75015, France
[5]Present address: Department of Ecology and Evolution, University of Chicago, Chicago, IL 60637, USA
[6]Present address: Institute of Molecular and Cell Biology, Proteos, Singapore 138673, Singapore

the cortex-inner coat interface [25, 26]. We examined the localization of our 40 coat protein-GFP fusions in the *safA* mutant background and identified 16 fusions that were impaired in localization (Figures 1A–1D and Figure S1). Thus, it appears that SafA is the major inner coat morphogenetic protein. In total, we define three genetic interaction subnetworks within the coat (Figure 1E): the *cotE*-dependent outer coat, the *safA*-dependent inner coat, and a third group independent of *cotE* and *safA*. The proteins of this third group genetically interact solely with *spoIVA* and *spoVM*.

The *B. subtilis* Spore Coat High-Resolution Physical Map

The modularity of the genetic interaction network supports the idea that individual coat proteins occupy distinct spatial regions of the coat. EM observations suggest that the coat width varies between 60 and 250 nm [15, 16], which overlaps with the theoretical limit of resolution of light microscopy [9]. We chose to measure the spatial localization of individual coat proteins with PSICIC, an algorithm that increases effective image resolution through interpolated contouring of conventional fluorescence microscopy images [12]. We used the forespore membranes [27] as a reference for all of our measurements. All p values quoted below are from the Wilcoxon rank-sum test.

We first tested our ability to distinguish between the inner coat protein, SpoVID-CFP, and the outer coat protein, CotE-YFP, in the same cell (Figure S2). Distributions of the measurements of distances from the membrane to each of the two fusions were significantly separated ($p = 4.3 \times 10^{-11}$). We extended these experiments to a set of 17 coat protein-GFP fusions representing all three genetic interaction classes (Figure 2A and Table S2). Without exception, the means of the measured distances correlated with the data from the genetic analysis. Using a significance cutoff of $p \leq 10^{-4}$, we define four spatially separated layers of proteins. Among the *cotE*-independent GFP fusions, the *safA*-independent fusions are not significantly separated from GFP-SpoIVA ($p > 0.02$), whereas all of the *safA*-dependent fusions are significantly separated ($7.5 \times 10^{-4} < p < 4.4 \times 10^{-9}$). These data suggest that SpoVM, SpoIVA, SpoVID, and YhaX form an innermost coat layer that is spatially distinct from the *safA*-dependent proteins CotD, CotT, YaaH, and YuzC. Wilcoxon tests against the CotE-GFP distribution suggest two spatially distinct layers within the outer coat as well. CotA, CotS, CotO, CotM, and YtxO are not significantly separated ($5.0 \times 10^{-3} < p < 0.77$). Intriguingly, CotG, CotW, and CotZ ($7.7 \times 10^{-7} < p < 4.7 \times 10^{-10}$) are separated, which suggests that they are present at the outermost surface of the coat.

We integrated our genetic interaction data with the PSICIC measurements by creating a distance-weighted interaction map (Figure 2B). From these data, we propose the existence of four spatially distinct coat layers: (1) an innermost layer containing the *cotE*- and *safA*-independent proteins; (2) an inner coat layer containing the *safA*-dependent proteins; (3) the *cotE*-dependent outer coat; and (4) a layer of *cotE*-dependent proteins at the outermost spore periphery. A recent study used a similar technique to suggest that the coat may be made up of more than two layers [28]. We cannot exclude the possibility that some coat proteins reside in multiple layers, particularly proteins with extended domains. It may be informative to compare the localization of proteins labeled at both termini and between structural domains to determine protein orientation [4]. Taken in total, these data suggest that the underlying genetic assumptions are correct.

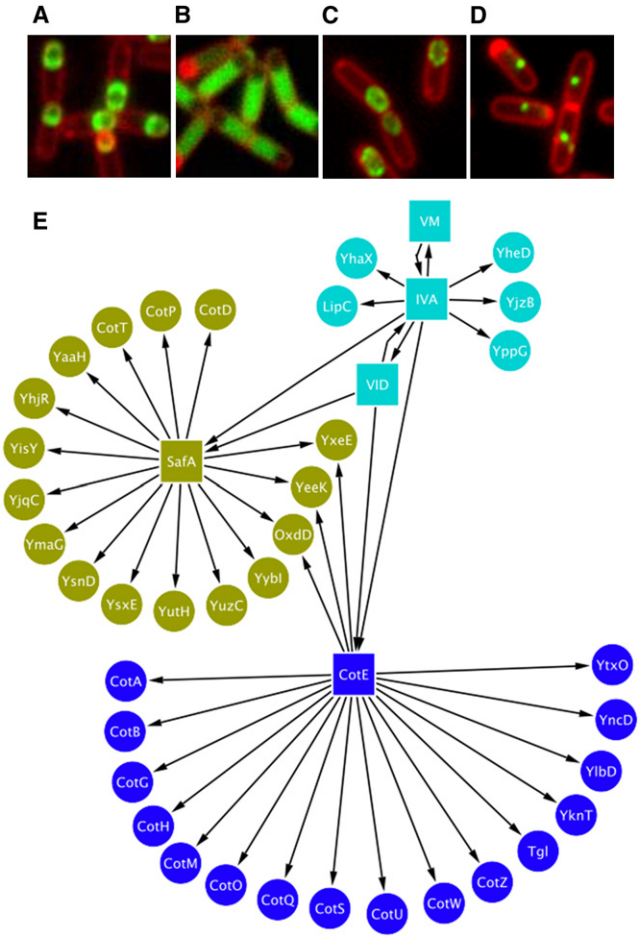

Figure 1. The Spore Coat Genetic Interaction Network

Examples of fluorescence microscopy images used in construction of the network. Cells were sporulated at 37°C by suspension in Sterlini-Mandelstam medium, stained with membrane stain (FM4-64, Invitrogen, red), and imaged 3 hr after resuspension. GFP-fusion fluorescence is shown in green.
(A) Cells contain *yaaH* fused to *gfp* (PE793).
(B) Cells contain *yaaH* fused to *gfp*, and *safA* is deleted (PE861). YaaH-GFP shows complete mislocalization in *safA* mutant cells.
(C) Cells contain *oxdD* fused to *gfp* (PE634).
(D) Cells contain *oxdD* fused to *gfp*, and *safA* is deleted (PE816). OxdD-GFP shows incomplete localization in *safA* mutant cells, forming a single dot.
(E) The spore coat interaction network was drawn in Cytoscape with directional edges (arrows) denoting genetic dependencies among genes and fusion proteins. The *safA*-dependency data were collected in this study. The remainder of the data is shown in Figure S1. Other genetic interactions were curated from the literature (Table S1).

The Outermost Layer of the *B. subtilis* Spore Coat

Our finding that CotG-GFP, CotW-GFP, and CotZ-GFP are present in an outermost coat layer led us to look for potential genetic interactions among these three proteins. In a mutant lacking *cotXYZ*, CotW-GFP completely fails to localize (Figure 3A). The mislocalization of CotW-GFP in the *cotXYZ* deletion and the positions of both CotW-GFP and CotZ-GFP within the outermost layer implied that *cotXYZ* mutant spores may have defective surfaces, as also suggested by previous studies of the *cotXYZ* mutant [29]. The application of Ruthenium red staining to EM has recently revealed an additional outermost layer of the coat that was undetectable in conventionally stained EMs [30]. Ruthenium red is a relatively promiscuous stain that binds sugars, free amino acids, some

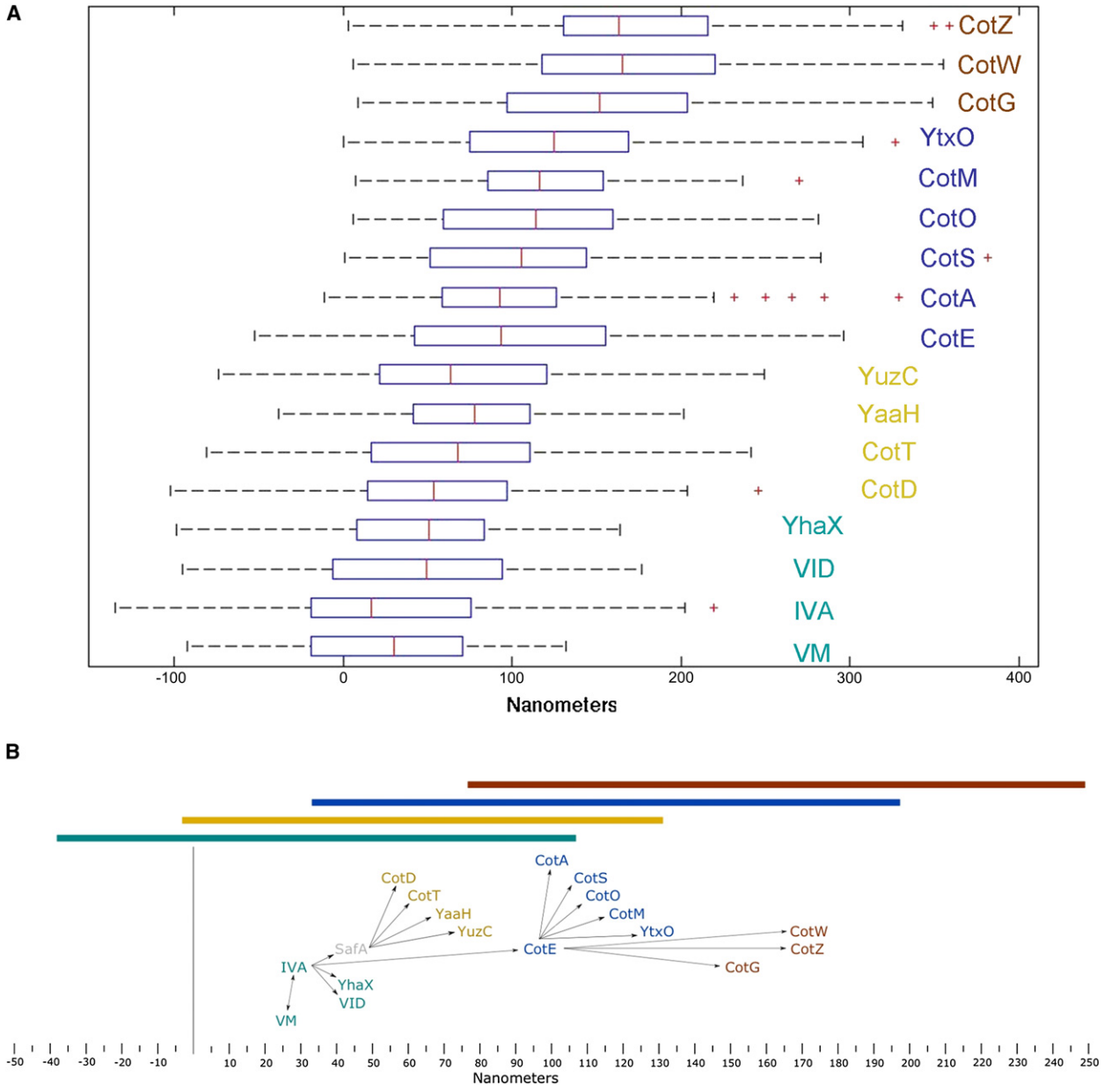

Figure 2. A Distance-Weighted Genetic Interaction Network

(A) Cells were sporulated by suspension in Sterlini-Mandelstam medium in the presence of Mitotracker Red (Invitrogen). Samples were collected at hour 6, pelleted, resuspended in PBS containing 1 $\mu g/mL^{-1}$ Mitotracker Red, and imaged by phase contrast and fluorescence microscopy. Five-section z-series spaced 0.3 μm apart were collected. Images were taken using brightfield with phase contrast and epifluorescence with TexasRed and FITC fluorescence filters at each z-step. Stacks were deconvolved for 30 iterations using Autoquant. The middle plane of each stack was analyzed with PSICIC to determine cell contours and to measure the location of the membranes and the fluorescent protein fusions within each cell. All strains are C-terminal GFP fusions, except SpoIVA (GFP-SpoIVA), which is fused at the N terminus. CotA (CotA-YFP) is a C-terminal YFP fusion. All fusions are integrated at the endogenous locus and are expressed from the native promoter, except *gfp-spoIVA* and *cotG-gfp*, which are integrated at the *amyE* locus and expressed from cloned *spoIVA* and *cotG* promoters respectively. All fusions are expressed in otherwise wild-type cells. Each box is delimited by the first and third quartiles, and the red line crossing the box is the median. The whiskers correspond to ±2.7 standard deviations. Crosses indicate outliers. Data and statistics are included in Table S2.
(B) Network of genetic interactions with distance-weighted edges. Edges in the network diagram represent genetic interactions found in fluorescence microscopy-based molecular epistasis experiments. Text boxes contain the names of coat proteins and are centered on the mean of the measurements from the membrane peak (MP) to the coat protein-GFP fusion at hour 6 of sporulation (Table S2) on the x axis. The y axis at 0 nm represents the MP. Position along the y axis is arbitrary. The colored bars above the diagram represent the total spread of data plus and minus one standard deviation from the means of all the members of the corresponding coat layer. The bars represent the *safA*-independent *cotE*-independent innermost coat layer (IVA, VM, VID, and YhaX) in cyan, the *safA*-dependent inner coat (CotD, CotT, YaaH, and YuzC) in gold, the *cotE*-dependent outer coat (CotA, CotS, CotO, CotM, and YtxO) in blue, and the *cotE*-dependent crust (CotG, CotW, and CotZ) in brown. The diagram was drawn with Inkscape and an original scale of 1 mm = 1 nm.

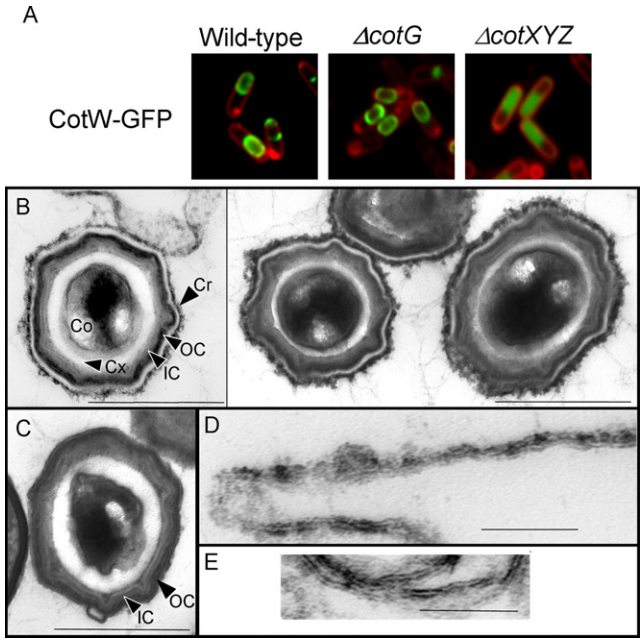

Figure 3. Characterization of the Outermost Coat Layer

(A) Cells were sporulated at 37°C by suspension in Sterlini-Mandelstam medium, stained with membrane stain (FM4-64, red), and analyzed by fluorescence microscopy at hour 5. One representative field of cells is shown for each condition. The image combines signal from the TexasRed and FITC channels. All strains express *cotW-gfp* from the endogenous locus. From left to right: CotW-GFP in an otherwise wild-type strain (PE599), CotW-GFP in a *cotG*::*erm* strain (PE2220), and CotW-GFP in a *cotXYZ*::*neo* strain (PE2224).

(B–E) Wild-type (B and D) and *cotXYZ* mutant (C and E) spores were fixed and stained with Ruthenium red and analyzed by thin-section transmission electron microscopy. The core, cortex, inner coat, outer coat, and crust are labeled (Co, Cx, IC, OC, and Cr, respectively). (D) and (E) show crust layer material not associated with a spore. The size bars are 500 nm (in B and C) or 100 nm (in D and E).

proteins, and lipids [31]; therefore, the composition of this surface layer remains unknown.

We used Ruthenium Red staining to examine wild-type and *cotXYZ* mutant spores. As previously reported [30], wild-type spores possess an additional electron-dense layer immediately outside the outer coat that is not present in spores stained conventionally (Figures 3B and 3D), which we name the crust. A gap between this layer and the outer coat surface is readily apparent. Ruthenium red staining revealed that the crust is absent from *cotXYZ* spores (Figure 3C). Instead, similar structures are present as misassembled material in the milieu (Figure 3E). Therefore, CotX, CotY, and/or CotZ play a morphogenetic role in the assembly of the crust around the spore. Because CotW-GFP is in the outermost layer and fails to localize in *cotXYZ* mutant spores, CotW is likely to be part of the crust. The simplest interpretation of these data is that the crust is composed of protein in addition to polysaccharide. Taken together, our data suggest the existence of a glycoprotein outermost layer of *B. subtilis* spores that requires *cotXYZ* for its deposition around the spore.

Conclusions

We found a surprising amount of modularity in the genetic interaction network. It appears that most coat proteins assemble under the control of only one of the major morphogenetic proteins. Because SpoIVA, SafA, CotE and CotY/CotZ have all been shown to multimerize in vitro [32–35], a possible mode of assembly for each layer may be polymerization of a basement layer made up of a morphogenetic protein and localization of other coat proteins onto that substratum.

Our data also suggest a major difference between assembly of the coat and of the bacterial flagellum. Flagella are built by integrating temporal control of a transcriptional cascade with morphogenetic checkpoints to ensure that the basal body is assembled before the hook and filament [6], resulting in a structure that is built up component by component. Intuitively, a concentrically layered spherical structure such as the coat would be most easily assembled layer by layer, from inside to outside. Among the early-expressed proteins, three localize to the outer coat (CotE, CotO, and CotM), and two localize to the crust (CotW and CotZ). These data suggest a large amount of simultaneous assembly of all coat layers. We propose that coat assembly begins with the asymmetric localization of a scaffold of all four layers to the mother cell-proximal pole of the spore surface. This may be followed by temporally distinct waves of encasement to complete the structure [10, 24]. Also, we find that two late-expressed coat proteins are part of the inner coat (CotD and CotT), implying that the inner layer is accessible to molecules as large as GFP-fusion proteins until quite late in coat morphogenesis.

It is now clear that both *B. subtilis* and *Bacillus anthracis* spores have glycoprotein layers as their surfaces [30]. Variation between species in the protein and sugar components of these outermost spore surfaces is likely to be critical in defining the ecological niches of spores and the chemical properties of the spore surface [36]. The spore crust identified here is not the equivalent of the exosporium of other spore-forming species [15, 17]. Although the outermost surface of the *B. anthracis* spore is the exosporium, a structure equivalent to the crust may also be present. Support for this comes from a recent crystallography study identifying a layer, possibly originating from the *B. anthracis* coat surface [37], which has intriguing similarities to features of the *B. subtilis* spore surface seen in freeze-etching studies [38]. ExsY, a CotZ homolog, was found in extracts of the *B. anthracis* exosporium [39]. On *exsY* mutant spores, the exosporium assembles on the mother cell–proximal pole of the spore but fails to encase the spore [40]. It is still unknown whether ExsY is a bona fide component of the exosporium or whether it localizes to the surface of the coat like its *B. subtilis* homolog.

Similar approaches to those taken here could be used in other well-described model systems. PSICIC could be used in a similar fashion as our study to measure the location of individual proteins relative to a stationary marker. Importantly, PSICIC can also reveal the temporal dynamics of protein localization at high resolution. The approach used here can be used to assist in ordering network connections to create models truer to the dynamics of life in three-dimensional space over time.

Experimental Procedures

Detailed experimental procedures are provided in the Supplemental Information. All *B. subtilis* strains are derivatives of PY79 [41] and are listed in Table S3. Fluorescence microscopy and sporulation by resuspension was performed as described elsewhere [23]. Fluorescence microscopy images were analyzed with PSICIC [12]. EM was performed as described in [42].

Supplemental Information

Supplemental Information includes two figures, three tables, and Supplemental Experimental Procedures and can be found with this article online at doi:10.1016/j.cub.2010.03.060.

Acknowledgments

We are grateful to Jonathan Dworkin, Adriano Henriques, and Rich Losick for comments on the manuscript and strains and to Anita Fernandez, David Gresham, Jake Jacobs, David Jukam, Kumaran Ramamurthi, and Pranidhi Sood for critical reading of manuscript. We acknowledge the financial support of the National Institutes of Health grant GM081571 to P.E., Department of the Army award number W81XWH-04-1-0307 to P.E., and training grant in Developmental Genetics 5T32HD007520 to P.T.M. The content of this material does not necessarily reflect the position or the policy of the U.S. government, and no official endorsement should be inferred.

Received: December 5, 2009
Revised: March 18, 2010
Accepted: March 19, 2010
Published online: May 6, 2010

References

1. Robinson, C.V., Sali, A., and Baumeister, W. (2007). The molecular sociology of the cell. Nature *450*, 973–982.
2. Alber, F., Dokudovskaya, S., Veenhoff, L.M., Zhang, W., Kipper, J., Devos, D., Suprapto, A., Karni-Schmidt, O., Williams, R., Chait, B.T., et al. (2007). The molecular architecture of the nuclear pore complex. Nature *450*, 695–701.
3. Schmid, E.M., and McMahon, H.T. (2007). Integrating molecular and network biology to decode endocytosis. Nature *448*, 883–888.
4. Joglekar, A.P., Bloom, K., and Salmon, E.D. (2009). *In vivo* protein architecture of the eukaryotic kinetochore with nanometer scale accuracy. Curr. Biol. *19*, 694–699.
5. Shapiro, L., McAdams, H.H., and Losick, R. (2009). Why and how bacteria localize proteins. Science *326*, 1225–1228.
6. Chevance, F.F., and Hughes, K.T. (2008). Coordinating assembly of a bacterial macromolecular machine. Nat. Rev. Microbiol. *6*, 455–465.
7. Adams, D.W., and Errington, J. (2009). Bacterial cell division: Assembly, maintenance and disassembly of the Z ring. Nat. Rev. Microbiol. *7*, 642–653.
8. Kramer, N., Hahn, J., and Dubnau, D. (2007). Multiple interactions among the competence proteins of *Bacillus subtilis*. Mol. Microbiol. *65*, 454–464.
9. Gitai, Z. (2009). New fluorescence microscopy methods for microbiology: Sharper, faster, and quantitative. Curr. Opin. Microbiol. *12*, 341–346.
10. Driks, A., Roels, S., Beall, B., Moran, C.P., Jr., and Losick, R. (1994). Subcellular localization of proteins involved in the assembly of the spore coat of *Bacillus subtilis*. Genes Dev. *8*, 234–244.
11. Rout, M.P., Aitchison, J.D., Suprapto, A., Hjertaas, K., Zhao, Y., and Chait, B.T. (2000). The yeast nuclear pore complex: Composition, architecture, and transport mechanism. J. Cell Biol. *148*, 635–651.
12. Guberman, J.M., Fay, A., Dworkin, J., Wingreen, N.S., and Gitai, Z. (2008). PSICIC: Noise and asymmetry in bacterial division revealed by computational image analysis at sub-pixel resolution. PLoS Comput. Biol. *4*, e1000233.
13. Reshes, G., Vanounou, S., Fishov, I., and Feingold, M. (2008). Cell shape dynamics in *Escherichia coli*. Biophys. J. *94*, 251–264.
14. Piggot, P.J., and Hilbert, D.W. (2004). Sporulation of *Bacillus subtilis*. Curr. Opin. Microbiol. *7*, 579–586.
15. Henriques, A.O., and Moran, C.P., Jr. (2007). Structure, assembly, and function of the spore surface layers. Annu. Rev. Microbiol. *61*, 555–588.
16. Driks, A. (1999). *Bacillus subtilis* spore coat. Microbiol. Mol. Biol. Rev. *63*, 1–20.
17. Driks, A. (2009). The *Bacillus anthracis* spore. Mol. Aspects Med. *30*, 368–373.
18. Warth, A.D., Ohye, D.F., and Murrell, W.G. (1963). The composition and structure of bacterial spores. J. Cell Biol. *16*, 579–592.
19. Piggot, P.J., and Coote, J.G. (1976). Genetic aspects of bacterial endospore formation. Bacteriol. Rev. *40*, 908–962.
20. Ramamurthi, K.S., Lecuyer, S., Stone, H.A., and Losick, R. (2009). Geometric cue for protein localization in a bacterium. Science *323*, 1354–1357.
21. Zheng, L.B., Donovan, W.P., Fitz-James, P.C., and Losick, R. (1988). Gene encoding a morphogenic protein required in the assembly of the outer coat of the *Bacillus subtilis* endospore. Genes Dev. *2*, 1047–1054.
22. Webb, C.D., Decatur, A., Teleman, A., and Losick, R. (1995). Use of green fluorescent protein for visualization of cell-specific gene expression and subcellular protein localization during sporulation in *Bacillus subtilis*. J. Bacteriol. *177*, 5906–5911.
23. Kim, H., Hahn, M., Grabowski, P., McPherson, D.C., Otte, M.M., Wang, R., Ferguson, C.C., Eichenberger, P., and Driks, A. (2006). The *Bacillus subtilis* spore coat protein interaction network. Mol. Microbiol. *59*, 487–502.
24. Wang, K.H., Isidro, A.L., Domingues, L., Eskandarian, H.A., McKenney, P.T., Drew, K., Grabowski, P., Chua, M.H., Barry, S.N., Guan, M., et al. (2009). The coat morphogenetic protein SpoVID is necessary for spore encasement in *Bacillus subtilis*. Mol. Microbiol. *74*, 634–649.
25. Ozin, A.J., Henriques, A.O., Yi, H., and Moran, C.P., Jr. (2000). Morphogenetic proteins SpoVID and SafA form a complex during assembly of the *Bacillus subtilis* spore coat. J. Bacteriol. *182*, 1828–1833.
26. Takamatsu, H., Kodama, T., Nakayama, T., and Watabe, K. (1999). Characterization of the *yrbA* gene of *Bacillus subtilis*, involved in resistance and germination of spores. J. Bacteriol. *181*, 4986–4994.
27. Sharp, M.D., and Pogliano, K. (1999). An *in vivo* membrane fusion assay implicates SpoIIIE in the final stages of engulfment during *Bacillus subtilis* sporulation. Proc. Natl. Acad. Sci. USA *96*, 14553–14558.
28. Imamura, D., Kuwana, R., Takamatsu, H., and Watabe, K. (2010). Localization of proteins to different layers and regions of *Bacillus subtilis* spore coats. J. Bacteriol. *192*, 518–524.
29. Zhang, J., Fitz-James, P.C., and Aronson, A.I. (1993). Cloning and characterization of a cluster of genes encoding polypeptides present in the insoluble fraction of the spore coat of *Bacillus subtilis*. J. Bacteriol. *175*, 3757–3766.
30. Waller, L.N., Fox, N., Fox, K.F., Fox, A., and Price, R.L. (2004). Ruthenium red staining for ultrastructural visualization of a glycoprotein layer surrounding the spore of *Bacillus anthracis* and *Bacillus subtilis*. J. Microbiol. Methods *58*, 23–30.
31. Luft, J.H. (1971). Ruthenium red and violet. I. Chemistry, purification, methods of use for electron microscopy and mechanism of action. Anat. Rec. *171*, 347–368.
32. Ramamurthi, K.S., and Losick, R. (2008). ATP-driven self-assembly of a morphogenetic protein in *Bacillus subtilis*. Mol. Cell *31*, 406–414.
33. Little, S., and Driks, A. (2001). Functional analysis of the *Bacillus subtilis* morphogenetic spore coat protein CotE. Mol. Microbiol. *42*, 1107–1120.
34. Ozin, A.J., Samford, C.S., Henriques, A.O., and Moran, C.P., Jr. (2001). SpoVID guides SafA to the spore coat in *Bacillus subtilis*. J. Bacteriol. *183*, 3041–3049.
35. Krajcikova, D., Lukacova, M., Mullerova, D., Cutting, S.M., and Barak, I. (2009). Searching for protein-protein interactions within the *Bacillus subtilis* spore coat. J. Bacteriol. *191*, 3212–3219.
36. Chen, G., Driks, A., Tawfiq, K., Mallozzi, M., and Patil, S. (2010). *Bacillus anthracis* and *Bacillus subtilis* spore surface properties and transport. Colloids Surf. B Biointerfaces *76*, 512–518.
37. Ball, D.A., Taylor, R., Todd, S.J., Redmond, C., Couture-Tosi, E., Sylvestre, P., Moir, A., and Bullough, P.A. (2008). Structure of the exosporium and sublayers of spores of the *Bacillus cereus* family revealed by electron crystallography. Mol. Microbiol. *68*, 947–958.
38. Aronson, A.I., and Fitz-James, P. (1976). Structure and morphogenesis of the bacterial spore coat. Bacteriol. Rev. *40*, 360–402.
39. Redmond, C., Baillie, L.W., Hibbs, S., Moir, A.J., and Moir, A. (2004). Identification of proteins in the exosporium of *Bacillus anthracis*. Microbiology *150*, 355–363.
40. Boydston, J.A., Yue, L., Kearney, J.F., and Turnbough, C.L., Jr. (2006). The ExsY protein is required for complete formation of the exosporium of *Bacillus anthracis*. J. Bacteriol. *188*, 7440–7448.
41. Youngman, P., Perkins, J.B., and Losick, R. (1984). Construction of a cloning site near one end of *Tn917* into which foreign DNA may be inserted without affecting transposition in *Bacillus subtilis* or expression of the transposon-borne erm gene. Plasmid *12*, 1–9.
42. Waller, L.N., Stump, M.J., Fox, K.F., Harley, W.M., Fox, A., Stewart, G.C., and Shahgholi, M. (2005). Identification of a second collagen-like glycoprotein produced by *Bacillus anthracis* and demonstration of associated spore-specific sugars. J. Bacteriol. *187*, 4592–4597.